

Supporting Information

A robust and renewable solar steam generator for high concentration dye wastewater purification

Xuan Wang, Kang Liu, Zubin Wang, Liping Heng,* and Lei Jiang

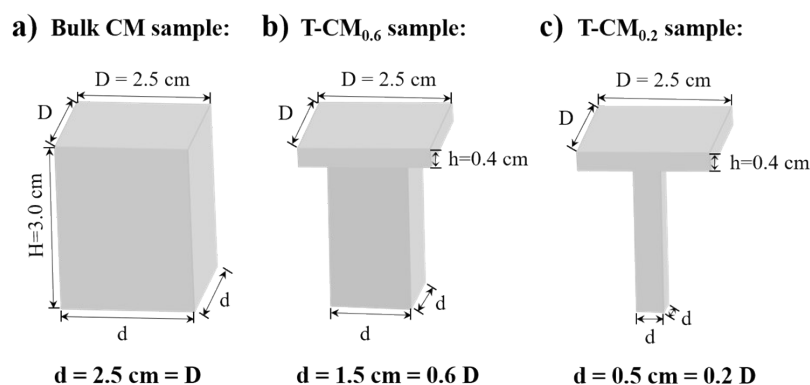


Figure S1. The schematic of a) bulk CM, b) T-CM_{0.6} and c) T-CM_{0.2} samples.

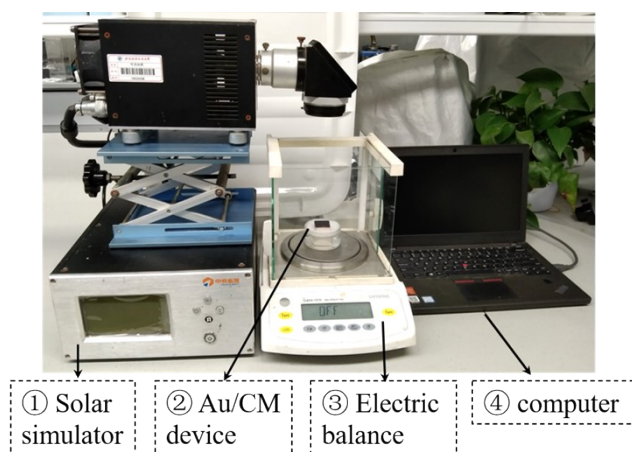


Figure S2. The setup diagram of solar steam generating system.

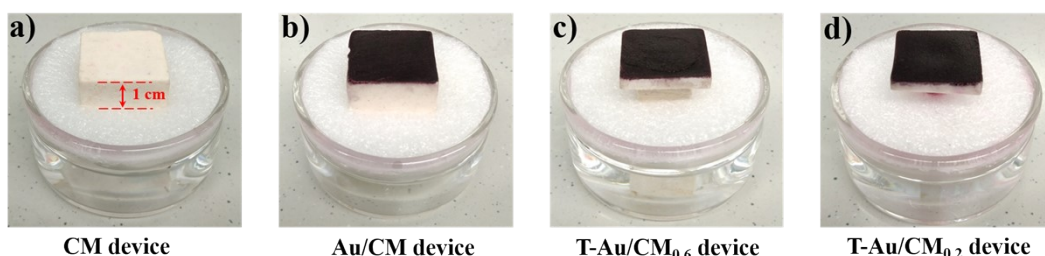


Figure S3. Photos of different evaporation devices including a) CM-only, b) bulk Au/CM, c) T-Au/CM_{0.6} and d) T-Au/CM_{0.2} devices.

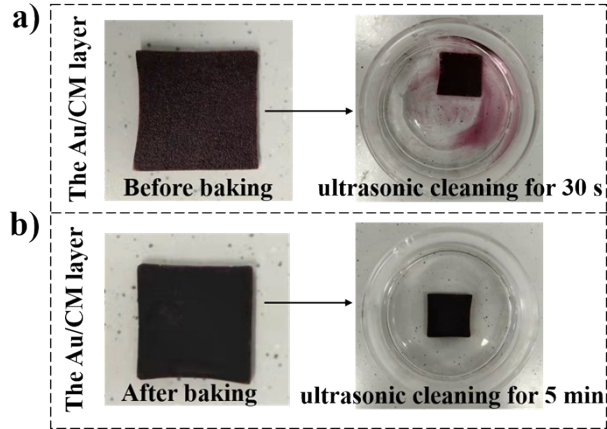


Figure S4. a) The Au/CM layer before baking are too incompact to resist the ultrasonic cleaning within 30s. b) In contrast, the prepared Au/CM layer after baking can keep its integrity even be ultrasonic cleaned for 5 min. To clearly observe the effect of ultrasonic cleaning, the Au nanoparticles were deposited on a thin CM layer with a 3 mm thickness.

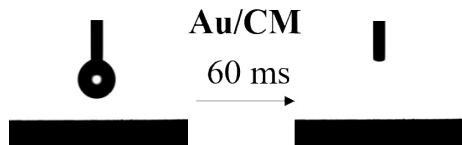


Figure S5. Images of dynamic water contact angle on the upper surface of Au/CM layer, exhibiting the Au/CM surface also possesses good superhydrophily.

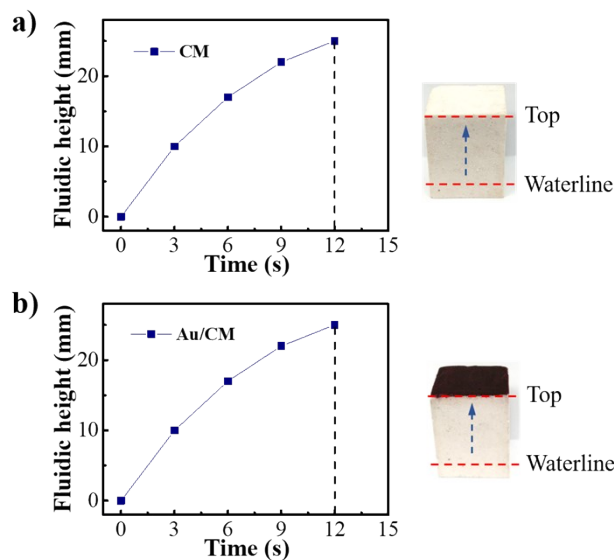


Figure S6. The water transportation capacity from waterline to the top surface (the direction of blue arrow) for a) bulk CM and b) Au/CM samples, when their bottom was immersed in water for 5 mm depth.

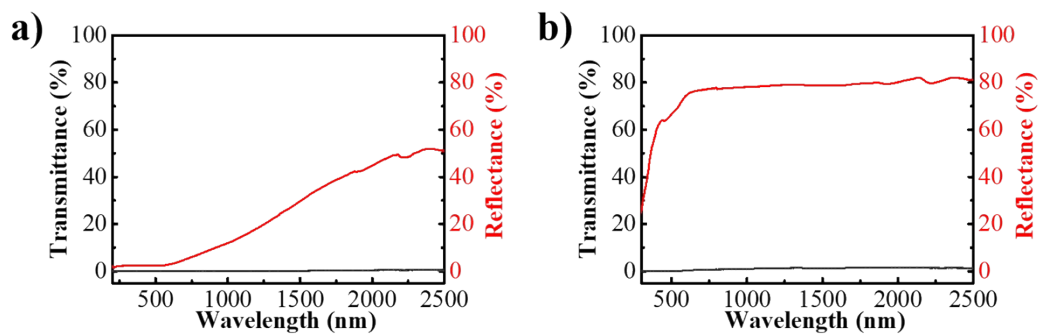


Figure S7. The transmittance and reflectance spectra of (a) Au/CM layer and (b) CM layer.

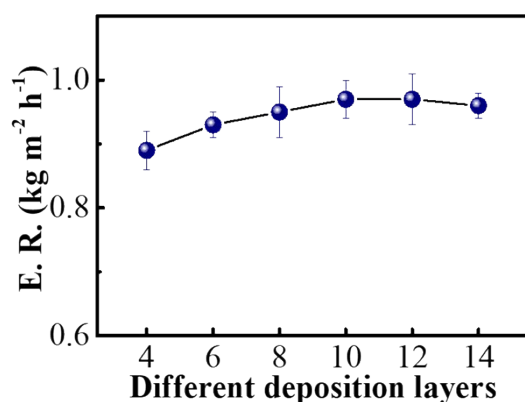


Figure S8. The influence of different Au nanoparticles deposition layers on the evaporation rate.

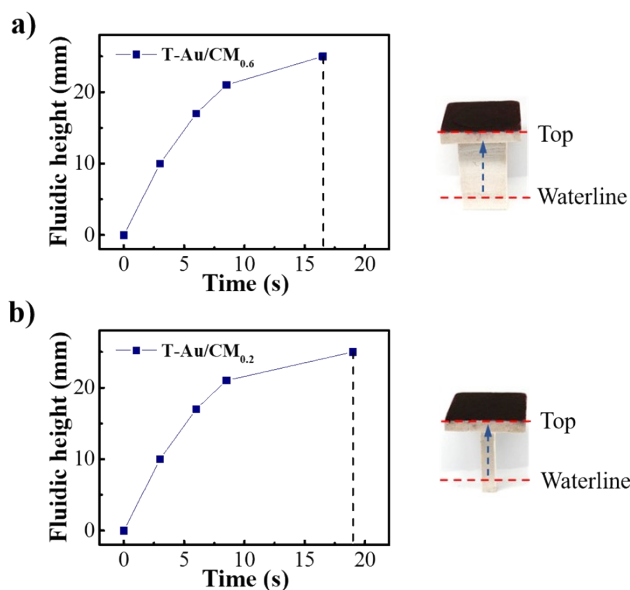


Figure S9. The water transportation capacity from waterline to the top surface (the direction of blue arrow) for a) T-Au/CM_{0.6} and b) T-Au/CM_{0.2} samples, when their bottom was immersed in water for 5 mm depth.

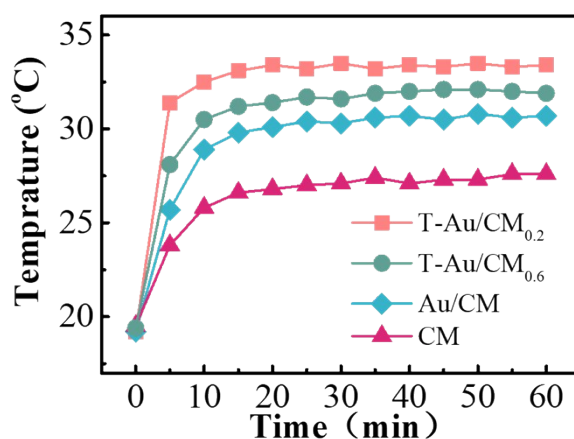


Figure S10. Surface temperature changes of four kinds of solar evaporation devices with increasing time in water evaporation process under 1-sunlight irradiation.

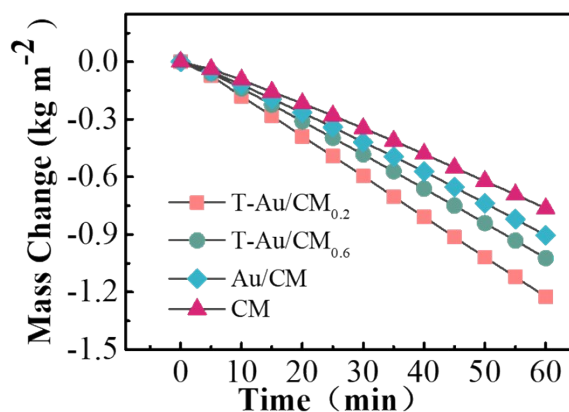


Figure S11. Comparison of the water mass change with time for different evaporation systems including CM-only, bulk Au/CM, T-Au/CM_{0.6} and T-Au/CM_{0.2} devices under 1-sunlight irradiation, respectively.



Figure S12. The condensation and collection of steam generated from T-Au/CM_{0.2} device under solar irradiation.

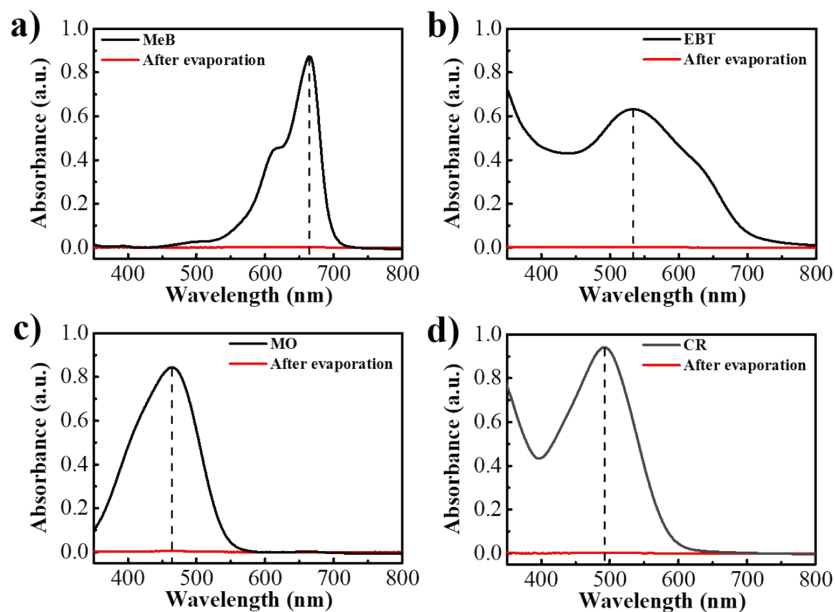


Figure S13. Absorption spectra of (a) MeB, (b) EBT, (c) MO and (d) CR reference solutions (black line), and corresponding condensed water after evaporation of T-Au/CM_{0.2} device (red line).

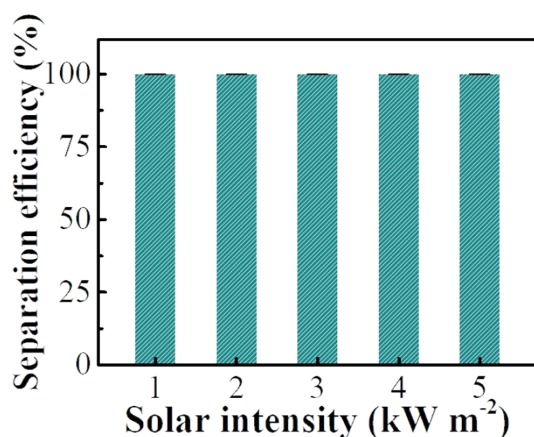


Figure S14. The separation efficiency of T-Au/CM_{0.2} device in separating 1 mg mL⁻¹ RhB wastewater, under different solar irradiation intensity.

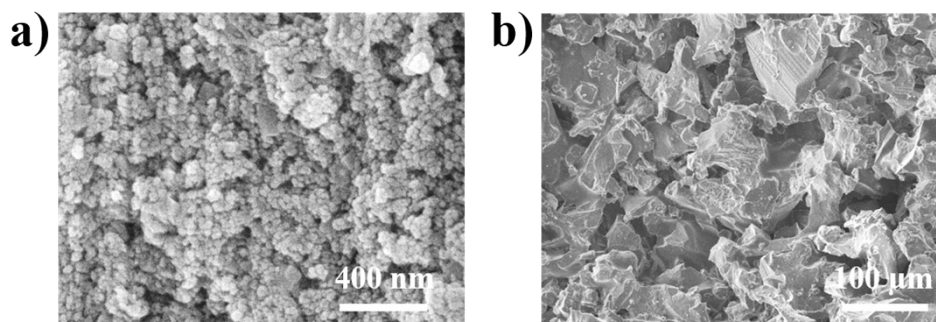


Figure S15. (a) The magnified SEM image of the upper Au layer after a 2 hours calcination at 600 °C. (b) The SEM image of the lateral CM layer after a 2 hours calcination at 600 °C.

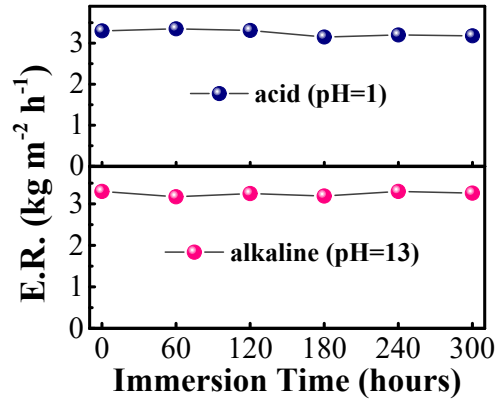


Figure S16. The evaporation rate changes of T-Au/CM_{0.2} device under 1-sunlight and 1 m s⁻¹ wind, after immersed in acid solution (pH=1) or alkaline solution (pH=13) for 300 hours.



Figure S17. The T-Au/CM_{0.2} sample withstanding a 500 g weight.

The calculation of solar evaporation efficiency:

Here, we calculate the corresponding solar evaporation efficiency (η_{ev}) for the devices in our work by the following expression:¹

$$\eta_{ev} = \frac{m(H_{LV} + Q)}{E_{in}} \quad (1)$$

$$H_{LV(T)} = 1.91846 \times 10^3 (T_1 - 33.91)^2 \quad (2)$$

$$Q = c(T_1 - T_0) \quad (3)$$

where m is the water evaporation rate under sunlight irradiation ($\text{kg m}^{-2} \text{h}^{-1}$), H_{LV} is the enthalpy of vaporization for water (kJ kg^{-1}), Q is the absorbed heat for water temperature increase (kJ kg^{-1}), E_{in} is the energy input of the incident sunlight ($\text{kJ m}^{-2} \text{h}^{-1}$), c is the specific heat capacity of water ($4.2 \text{ kJ kg}^{-1} \text{K}^{-1}$), T_1 is the temperature of evaporation interface (K), and T_0 is the original temperature of water (K). And the calculation of η_{ev} was exhibited in the following Table S1.

Table S1. The calculation of η_{ev} for different Au/CM devices.

Devices	m ($\text{kg m}^{-2} \text{h}^{-1}$)	T_1 (K)	T_0 (K)	E_{in} ($\text{kJ m}^{-2} \text{h}^{-1}$)	η_{ev}
bulk Au/CM	0.97	303.25	292.45	3600 (1-sunlight intensity)	66.7%
T-Au/CM _{0.6}	1.08	304.55			74.4%

T-Au/CM _{0.2}	1.26	306.55			87.0%
------------------------	------	--------	--	--	-------

Table S2. The detail values for the separation efficiency calculation of RhB wastewater with different concentration.

C_0 (mg mL ⁻¹)	C_r (mg mL ⁻¹)	A_r (a. u.)	A_p (a. u.)	$\frac{C_r A_p}{C_p = A_r}$	$\eta = \frac{C_0 - C_p}{C_0} \quad *$ 100%
0.01 (RhB)	0.004 (RhB)	0.696	0.00344	0.00002	99.80%
0.1 (RhB)			0.00382	0.00002	99.98%
1 (RhB)			0.00521	0.00003	~ 100.00%
10 (RhB)			0.00432	0.00002	~ 100.00%

Table S3. The detail values for the separation efficiency calculation of different types dye wastewater.

C_0 (mg mL ⁻¹)	C_r (mg mL ⁻¹)	A_r (a. u.)	A_p (a. u.)	$\frac{C_r A_p}{C_p = A_r}$	$\eta = \frac{C_0 - C_p}{C_0} \quad *$ 100%
1 (MeB)	0.01 (MeB)	0.873	0.00220	0.00003	~100.00%
1 (EBT)	0.04 (EBT)	0.632	0.00132	0.00008	99.99%
1 (MO)	0.01 (MO)	0.844	0.00403	0.00005	~100.00%
1 (CR)	0.02 (CR)	0.941	0.00131	0.00003	~100.00%

Reference

1 X. Wu, Z. Q. Wu, Y. D. Wang, T. Gao, Q. Li and H. L. Xu, *Adv. Sci.*, 2021, **8**, 2002501.